Characterization of Langmuir−Blodgett Films of a Ferroelectric Liquid Crystal

Zi Wen,[†] Qing Jiang,*[,†] Kenji Tatani,[‡] and Yukihiro Ozaki*[,‡]

Key Laboratory of Automobile Materials, Ministry of Education, Department of Materials Science and Engineering, Jilin University, Changchun 130025, China, and Department of Chemistry, School of Science and Technology, Kwansei-Gakuin University, Gakuen, Sanda, Hyogo 669-1337, Japan

Received: September 14, 2005; In Final Form: December 8, 2005

Molecular orientation, structure, and phase transition behaviors in Langmuir−Blodgett (LB) and cast films of a ferroelectric liquid crystal of *sec*-butyl 6-(4-(nonyloxy)benzoyloxy)-2-naphthoate (FLC-1) are determined by ultraviolet (UV) spectroscopy, X-ray diffraction, and infrared (IR) spectroscopy. It is found that the orientation angle of chromophores θ in LB films is 41° from the surface normal. The tilt angle of the chromophore changes at 56, 70, and 88 °C, respectively, which denotes the presence of phase transitions. Two kinds of layered or isomeric crystal structures of the LB films with layer spacings of 3 and 3.5 nm at room temperature have been found while the latter disappears above 45 °C, as confirmed by measurement of temperature-dependent IR spectra.

1. Introduction

Since Meyer et al. first reported the existence of ferroelectricity in liquid crystals in 1975,[1] many studies have committed themselves to potential application in the fields of nonlinear optics, information storage, and display devices of the liquid crystals since the liquid crystals have characteristics of fast electrooptic switching and optical bistability. The homogeneously unwound alignment of the helix of the Smectic C* phase (S_m-C*) in liquid crystals is an essential prerequisite for the appearance of ferroelectricity, which can be obtained by surface-stabilized ferroelectric liquid crystals (FLC)[2−4] due to the boundary effect. In the above applications, FLC in an isotropic phase is filled into a very thin sample cell to reveal spontaneous polarization where the cell consists of two plates coated with a conducting layer of indium tin oxide and an aligning film. The film is rubbed in one direction to anchor FLC molecules with a good orientation to the inside surface of the thin cell. Finding out an appropriate aligning film material and an aligning technique are important since the interaction between the FLC molecules and the aligning film plays an essential role on the electrooptic property. However, a cell with few defects and excellent electrooptic characteristics is difficult to obtain by rubbing polyimide films, obliquely evaporated SiO_2 films, or polyimide LB films.[5] Therefore, the manufacturing technique of large-scale thin liquid crystal cells is a key technique in the application to control molecular orientation and stability, and then to develop FLC films without liquid crystal cells.

To highly organize FLC molecules homogeneously and to form a uniform film with well-defined thickness and orientation in a cell, the LB technique has recently been used to control and build such supermolecular assemblies through a layer-by-layer deposition process.[6] Up to now, spread monolayers and transferred LB films of liquid crystals have been studied extensively.[7−14] The liquid crystals in the LB films exhibit ferroelectric polarization with faster switching than that in the corresponding bulk.[12] However, only a few studies have treated LB films of FLC.[8,11,13]

Recently, LB films of ferroelectric liquid crystals of *sec*-butyl 6-(4-(nonyloxy)benzoyloxy)-2-naphthoate (FLC-1) have been fabricated successfully and the primary results for the fabrication technique and IR spectroscopy characterization of FLC-1 films are described shortly.[15] Therein the fabricated LB films of FLC-1 have highly ordered crystal structure with a trans-zigzag alkyl chain and a hexagonal or analogous (pseudohexagonal) subcell packing.[15]

In this contribution, molecular orientation, structure, and thermal behavior in monolayer and multilayers of the LB films and related cast films are characterized. The results show that the chromophores of polymorphous FLC-1 in the LB films form H-aggregates with $\theta = 41°$. In addition, phase transition temperatures among different liquid crystal phases are determined.

2. Experimental Section

A Kyowa Kaimen Kagaku Model of the HBM-AP Langmuir trough with a Wihelmy balance was employed for the $\pi-A$ isotherm measurements and for the preparation of Z-type LB films. A chloroform solution (1.0×10^{-3} M) of FLC-1 was spread onto an aqueous subphase of water (>18.1 MΩ, pH 6.2), which was doubly distilled from deionized water. The temperature of the water subphase was kept at 18 °C. After evaporation of the solvent, monolayers were compressed at a constant rate of 30 $cm^2\ min^{-1}$ under a given surface pressure of 8 mN m^{-1} (collapse surface pressure is 12 mN m^{-1}). The $\pi-A$ isotherm of the spread monolayer showed that the monolayer is a condensed film under the surface pressure.[6] The monolayers were transferred under the given pressure by the vertical dipping method onto CaF_2 plates for IR transmission measurements. During the initial deposition process, the transfer of molecules on a plate remained good on the withdrawal but few molecules were transferred on the immersion and then the transfer ratio is 0.98, which implies that the FLC-1 forms Z-type LB films. When the layer number is 5 or more, the transfer ratio decreases slightly. The substrates used had been subjected to ultrasonification in acetone and then in chloroform.

* To whom correspondence should be addressed. E-mail: jiangq@jlu.edu.cn (Jiang), ozaki@kwansei.ac.jp (Ozaki).
[†] Jilin University.
[‡] Kwansei-Gakuin University.

10.1021/jp055195h CCC: $33.50
Published on Web 01/13/2006

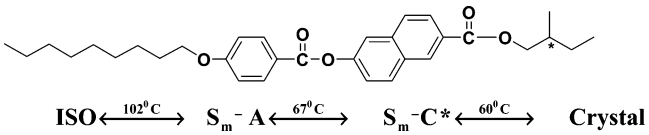

Figure 1. Structure and the phase transition temperatures of FLC-1.

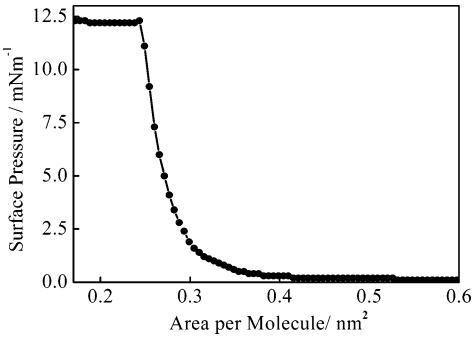

Figure 2. Surface pressure−area isotherm of FLC-1 on a pure water subphase at 18 °C

To prepare cast films of FLC-1, FLC-1 in chloroform with a concentration of 1.0×10^{-3} M was spread evenly onto a CaF_2 plate that first was ultrasonically cleaned. After the solvent was evaporated, the cast films with the substrate were dried in the atmosphere.

IR transmission was measured with a Thermo Nicolet Magna 550 FT-IR spectrometer equipped with a liquid nitrogen cooled MCT detector. The spectra were taken at a 4 cm^{-1} resolution and 256 interferograms were co-added to yield the spectra of a high signal-to-noise ratio.

Temperature-dependent UV−vis absorption spectra was recorded with a heating rate of 0.5 °C min^{-1} on a Shimadzu UV-3101 PC spectrophotometer, which was connected with a METTLER FP80HT temperature controller with error of ±0.05 °C, while LB films deposited on a CaF_2 plate were inserted into a sample holder.

The low-angle X-ray diffraction measurement was carried out with a Rigaku Rad-rb system (Cu $K\alpha_1$, 32 kV, 20 mA).

3. Results and Discussion

3.1. Fabrications of LB Films of FLC-1. Chemical structure and transition temperatures of synthesized bulk FLC-1[16] are shown in Figure 1.

As shown in the figure, as temperature increases, FLC-1 crystals melt at 102 °C. Between the crystal and the liquid, there are still two liquid crystal phases of S_m-C* and S_m-A (Smectic A). The corresponding transition temperatures are 60 and 67 °C, respectively.

Figure 2 shows a surface pressure−area (π−A) isotherm of FLC-1 on the pure water subphase. FLC-1 forms a condensed monolayer because it gives a sharp increase of the surface pressure in the range of 2.5−12 mN/m with a decrease of the single molecular area. The monolayer has a lower collapse surface pressure of 12 mN/m. On the other hand, the limiting area occupied by each molecule is estimated to be 0.286 nm^2 by extrapolating the sharp rising part of the π−A curve to zero surface pressure, which is a little larger than the limiting area of a stearic acid monolayer, suggesting that the molecular packing is loosely packed in the spread monolayer of FLC-1. This may be induced by the structure characteristic of FLC-1. The aggregation states and the tilt angles of the molecular axes of chromophores in LB films are affected by the number of carbon atoms in the tail (*l*) and the spacer (*m*) portions of the hydrophobic chain, the layer number, and the type of headgroup.[17,18] In general, the longer *l* or *m* is, the smaller is the tilt angle of the molecular axes in the LB films.[19] In the present case, $l = 9$, and another shorter tail *m*, being too short to leave and stand on the water subphase perpendicularly, exists at the other end. This arrangement leads to loose packing in the spread monolayer than the stearic acid. Thus, the area occupied by each molecule on the water subphase enlarges a little in comparison with the area occupied by a sample having a single alkyl chain or alkyl chains with the same length.

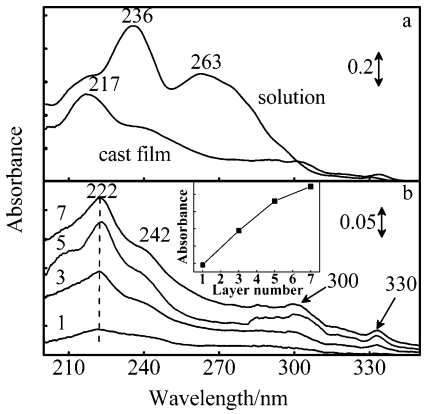

Figure 3. UV absorption spectra of FLC-1 measured at 25 °C for (a) a cast film with an acetonitrile solution (2×10^{-5} M) and (b) 1-, 3-, 5-, and 7-layer LB films deposited on CaF_2 plates. The insert shows the absorbance of the band at 222 nm versus the layer number of the LB films.

3.2. Aggregation and Orientation of the Chromophore in LB Films of FLC-1. Figure 3a shows UV spectra of a cast film of FLC-1 and that of an acetonitrile solution (2×10^{-5} M) of FLC-1, and Figure 3b depicts those of 1-, 3-, 5-, and 7-layer LB films of FLC-1 deposited on CaF_2 plates. The insert is the absorbance of the band at 222 nm versus the layer number of films of FLC-1. The absorbance of all LB films increases linearly with the layer number except for the 7-layer LB film, which deviates slightly from the straight line possibly due to its imperfection induced by the loss of some molecules during the deposition process, as stated in the Experimental Section. The spectrum of the acetonitrile solution of FLC-1 shows two absorption maxima at 236 and 263 nm, which are assigned to the $\pi-\pi^*$ transition of benzene and naphthalene rings in the FLC-1 chromophore. The two bands appear at 222 and 242 nm for $\pi-\pi^*$ transitions of the chromophore of LB films with blue shifts of about 14 and 21 nm compared with the corresponding band of the solution, whose transition moments are roughly perpendicular and parallel to the long axis of the chromophore, respectively.[20] New absorption bands appear at 300 and 330 nm, which are assigned to a $n-\pi^*$ transition of the C═O group of the chromophore.

According to the state interaction theory,[21,22] the exciton effects induced by the exciton splitting of excited states in a molecular aggregate may be observed if sufficiently strong electronic transitions exist in the monomer and if the interchromophore electron overlap is small in the molecular aggregate. Here a band shift is present. The amount of the wavelength shift, $\Delta\lambda$, is proportional to the energy of exciton splitting, ΔE, and the degree of aggregation. The blue shifts observed above are indicative of H-aggregate formation whose linear chromophore aggregate with their transition moments are parallel to each other and perpendicular to the stacking direction. Note that $\Delta E \propto 1/r^3$, where *r* is the distance of neighboring molecules.[22] Because *r* of the LB films is larger than the area

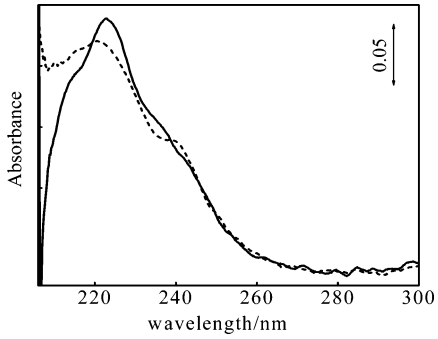

Figure 4. Polarized UV absorption spectra of a 5-layer LB film of FLC-1 at 25 °C. The solid and dotted lines indicate the s- and p-polarizations, respectively. The angle of incidence was 30°.

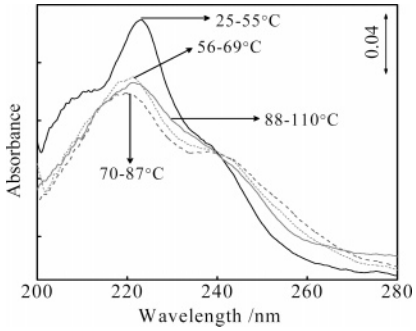

Figure 5. Ultraviolet absorption spectra of a 5-layer LB film of FLC-1 measured over a temperature range of 25 to 110 °C.

occupied by a stearic acid, a smaller blue shift is present due to the relationship of $\Delta E \propto \Delta\lambda$.

Figure 4 shows polarized UV absorption spectra of a 5-layer LB film of FLC-1. The band intensities A_P and A_S of the film were obtained after a baseline correction where subscripts P and S denote parallel and perpendicular polarization directions, respectively. The band at 222 nm in the S-polarization spectrum is stronger than that in the P-polarization one, while the band at 242 nm shows a reverse tendency.

If an angle between the uniaxial orientation of the transition moment and the surface normal is defined as θ' and an angle between the orientation of the transition moment and the long axis of chromophore is θ, when the transition moment is perpendicular or parallel to the long axis of the chromophore, $\theta' + \theta = 90°$ or $\theta' = \theta$. Thus, θ can be determined through evaluating θ', which can be determined by the measured ratio of A_P and A_S,[23,24]

$$\frac{A_P}{A_S} = \frac{n_1 \cos\theta_i + n_3 \cos\theta_r}{n_1 \cos\theta_r + n_3 \cos\theta_i}\left(\cos\theta_i \cos\theta_r + \frac{2{n_1}^3 n_3 \sin^2\theta_i}{{n_2}^4 \tan^2\theta'}\right) \quad (1)$$

where $n_1 = 1.00$,[25] $n_2 = 1.50$,[17,25] and $n_3 = 1.42$[25] are the refractive indices of air, the LB film, and CaF_2, respectively, $\theta_i = 30°$ is the incidence angle at the air/LB film interface, and $\theta_r = 20.6°$ is the angle of refraction at LB film/substrate determined by refraction law. Inserting $A_P = 0.27$ and $A_S = 0.29$ of the band at 222 nm and the above-mentioned parameters into eq 1, $\theta' = 49°$, which leads to $\theta = 41°$ due to the relationship of $\theta' + \theta = 90°$. This result implies that the medium strength H-aggregates are formed, which consequently bring out the presence of the medium-size blue shift of $\pi-\pi^*$ transition bands of the LB films.

3.3. Thermal Behavior of the Chromophoric Part in the LB Films of FLC-1. Figure 5 depicts temperature-dependent thermal behavior of the chromophoric parts in 5-layer LB films

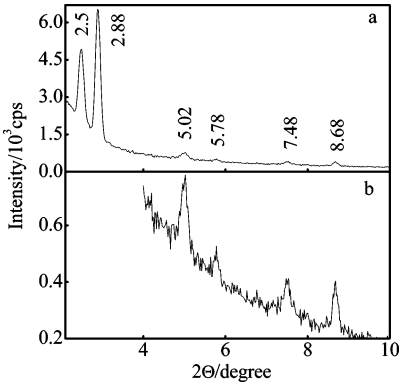

Figure 6. X-ray diffraction pattern of an 11-layer LB film of FLC-1 at room temperature (a) and the enlargement of weak peaks in the 4−10° region (b).

between 25 and 110 °C with an increment of 1 °C where the phase transitions occur at 56, 70, and 88 °C with changes of chromophore orientations rather than molecular aggregations. This is because there are significant intensity changes in two $\pi-\pi^*$ transition bands with small wavelength shifts. Referring to Figure 1, 56 and 70 °C correspond to the phase transitions from the crystal to S_m-C* and from S_m-C* to S_m-A, respectively.[26] However, the phase transition at 88 °C is absent in Figure 1 and should denote a new phase transition between the S_m-A phase and an isotropic phase. The intensity of the shorter wavelength band (222 nm) becomes weaker while that of the longer one (242 nm) is stronger at each phase transition temperature except at 88 °C where an opposite change is shown. Since the electric vector of the UV light is parallel to the substrate in the normal UV measurements, the band intensity change corresponds to that of θ' (or θ) only at phase transition temperatures where θ' deceases (or θ increases) after the first two phase transitions but in reverse at 88 °C.

In a transition between a crystal and a liquid crystal, the positional order is broken and orientational order is left.[27] Among different smectic liquid crystal phases, liquid crystal molecules are organized in a layered center-of-mass distribution. Within any given layer, a molecular long axis is strongly oriented along a certain direction, which is along the layer normal for the S_m-A phase, but has a tilt angle from the layer normal for the S_m-C* phase. Thus, the molecular long axis tends to orient perpendicularly to the substrate surface for the S_m-C*−S_m-A transition while θ increases as shown in Figure 5. This opposite tendency between the change of the molecule direction and that of θ indicates that there exists an angle between the long axis of the chromophore and that of the alkyl chain. Note that the band intensity at 88 °C is a little stronger than that at 70 °C (S_m-A), but is still weaker than that at 56 °C (S_m-C*). Thus, the newly appearing phase transition at 88 °C may correspond to the transition from S_m-A to the nematic liquid crystal phase (N phase) where the molecular orientations in both S_m-A and N phases are similar but the positional order is completely broken in the N phase. After this temperature, up to 110 °C, no drastic spectral change is found.

3.4. X-ray Diffraction Pattern. Figure 6 shows the X-ray diffraction pattern of a 11-layer LB film with CaF_2 substrate at room temperature. Peaks appear at $2\Theta = 2.50°$, 2.88°, 5.02°, 5.78°, 7.48°, and 8.68°. Since the structural requirements for observing several orders of X-ray diffractions are rather stringent, even a few interruptions in the layer structure, although leaving most of the structure intact, may cause a serious loss of phase coherence and X-ray intensity. Therefore, in low-angle X-ray diffraction experiments of LB films with low order, more

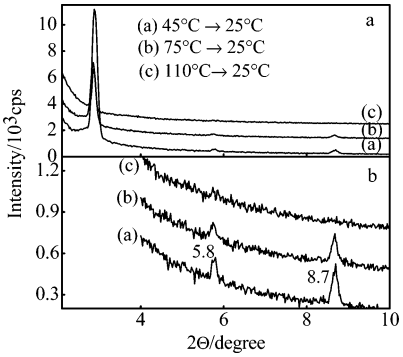

Figure 7. Annealing effects on the X-ray diffraction pattern of an 11-layer LB film of FLC-1 (a) and the enlargement of the weak peaks in the 4−10° region (b).

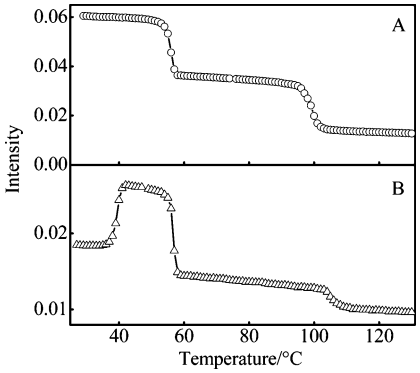

Figure 8. Temperature dependences of the peak intensities of the C═O stretching band of the part near the chiral carbon atom for the cast films (A) and 11-layer LB films (B) of FLC-1.

than one diffraction peak is seldom observed.[28] A calculation on the layer spacing (the *d* distance in the LB film) leads to the conclusion that the six peaks are attributed to two sets of diffraction angles or two kinds of isomeric crystal structures with $d = 3.0$ and 3.5 nm, respectively. If the film is heated, which is shown in Figure 7, only one set of diffraction pattern with $d = 3.0$ nm is left above 45 °C. When the temperature is raised to 75 °C, the diffraction peaks become weak, and disappear when the film is heated to isotropic temperature. Thus, $d = 3.5$ nm may denote an unknown metastable crystalline phase, which will be considered elsewhere.

3.5. Temperature-Dependent IR Studies in the LB and Cast Films of FLC-1. To further characterize the LB films of FLC-1, we have monitored the temperature-dependent IR spectral change by plotting the peak intensities of the C═O stretching band of the part near the chiral carbon atom between 20 and 130 °C with an increment of 1 deg for the 11-layer LB film and the cast film, which are shown in Figure 8. This is because IR spectroscopy is a powerful tool for exploring molecular structure and orientation in thin films through considering frequencies and intensities of the bands.[29,30] As shown in the figure, the 11-layer LB film gives three-step sharp spectral changes near 40, 56, and 104 °C, while the cast film undergoes two transition processes near 56 and 100 °C, respectively. Referring to Figure 1, the phase transition occurring near 56 and 100 or 104 °C may be ascribed to the phase transition between the crystal and S_m-C* and the melting of the alkyl chains into an isotropic state, respectively. However, the first transition occurring near 40 °C in the LB film should be a polymorphous transition. It is known that the polymorphous transition in cast films cannot be monitored by temperature-dependent IR possibly due to the overlapping of many bands in corresponding temperature regions. However, this transition

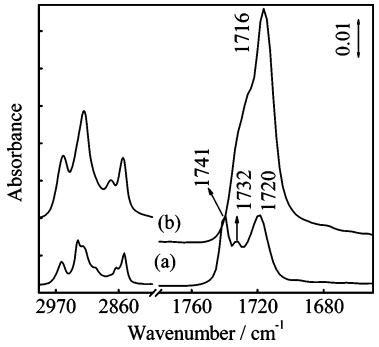

Figure 9. IR transmission spectra in the 3000−1650 cm^{-1} region of FLC-1 of (a) a 11-layer LB film and (b) a cast film.

near 40 °C can be clearly observed in the LB films, being in good agreement with the X-ray diffraction study for the thermal behavior discussed above. Thus, both techniques confirm the existence of a metastable crystalline phase in the FLC-1 crystal, which is difficult to find in bulk.

Such an isomeric crystal structure in FLC-1 is also reflected in IR spectra of LB films of Figure 9 where the C═O stretching band region of the LB film (the 1750−1700 cm^{-1} region) significantly differs from that of the cast film. The cast film gives bands at 1736 and 1716 cm^{-1} assigned to the C═O stretching modes of the core part and the part near the chiral carbon atom, respectively.[26] The LB film yields three bands at 1741, 1732, and 1720 cm^{-1} due to the C═O stretching modes, which implies that there are distinct rotational isomerism characteristics in the LB film due to the LB technique of the layer-by-layer deposition process. Moreover, the C═O stretching vibration in the RA spectra of LB films yields two bands,[15] but no band for the rotational isomerism due to the stronger interaction between the Au substrate and the C═O group at the chiral part in the first layer of the LB film, which in turn increases the absorbance of the C═O stretching vibration of the core part a little. As a result, the C═O stretching band of the core part of the LB films in the RA spectra is slightly stronger than that in the transmission spectra. The reverse is true for the one near the chiral carbon atom. Thus, the ordered multilayer LB films are characterized by retaining rotational isomerism while this is absent in cast films, which further supports the conclusion obtained from Figures 7 and 8 that FLC-1 possess a polymorphism structure.

3.6. Discussion on the Possible Application of LB Films of FLC-1. FLC-1 is characterized by having a bookshelf layer structure[16] for a particular alignment film in the Sm-C***** phase, which as a liquid crystal with a small molecular weight has a faster response speed than a polymer. Thus, it would be of interest to compare the electrooptic switching of LB films with that of a homotropically oriented bulk sample, which is a promising feature for possible applications of the LB film in this area.

However, it is clear that the aseismatic properties of FLC-1 are as good as that of polymers. Hence, a single FLC-1 film as panel display devices has not been utilized commercially at present while a composite consisting of liquid crystals and polymers prefers to be applied. Thus, the improvement of the aseismatic properties of FLC-1 will be a future task for its application.

4. Conclusions

The chromophores of FLC-1 LB films form H-aggregates with medium strength with $\theta = 41°$, being larger than the tilt angle of the alkyl chain. The phase transition of the crystal to

S_m-C* at 56 °C and that of S_m-C* to S_m-A phase at 70 °C are present while the phase transition near 88 °C has been attributed to a transition between S_m-A and the N phase. There are clear differences in the C═O stretching region of IR transition spectra between the LB and the cast films, which are induced by the existence of rotational isomerism around the O−C axis of the chiral part. Temperature-dependent spectral changes in the IR spectra and X-ray diffraction for 11-layer LB films of FLC-1 have revealed that the LB films possess a well-ordered layered structure, which have two kinds of isomeric crystalline structures where one of them is newly found. All these provide good clues for the optimization of the spontaneous polarization of a ferroelectric liquid crystalline film without external electric or magnetic fields and deepen our understanding for connecting molecular and macroscopic properties of organic materials.

Acknowledgment. One of the authors (Z.W.) thanks Kwansei-Gakuin University, Japan for providing the opportunity of staying there for the research. The authors have benefited from discussions with Prof. T. Hasegawa (Nihon University, Japan). We are grateful to Mr. Toshiaki Yoshihara (Fujitsu Laboratories Ltd., Akashi, Japan) for providing us with FLC-1. Wen and Jiang were supported by grants (No. 2004CB619301) from the National Key Basic Research and Development Program, China and by the "985 Project" of Jilin University. Ozaki was supported by a Grant-in-aid for Scientific Research (c) (No. 14540477) from the Ministry of Education, Culture, Sports, Science and Technology, Japan.

References and Notes

(1) Meyer, R.; Liébert, L.; Strzelecki, L.; Keller, P. *J. Phys. Lett.* **1975**, *L69*, 36.
(2) Clark, N. A.; Lagerwall, S. T. *Appl. Phys. Lett.* **1980**, *36*, 899.
(3) Clark, N. A.; Handschy, M. A.; Lagerwall, S. T. *Mol. Cryst. Liq. Cryst.* **1983**, *94*, 213.
(4) Beresnev, L. A.; Blinov, L. M.; Osipov, M. A.; Pikin, S. A. *Mol. Cryst. Liq. Cryst.* **1988**, 158A.
(5) Matsumoto, S.; Hatoh, H.; Kamagami, S.; Murayama, A. *Ferroelectrics* **1988**, *85*, 235.
(6) Roberts, G. G. *Langmuir−Blodgget Films*; Plenum Press: New York, 1990.
(7) Xue, J.; Jung, C. S.; Kim, M. W. *Phys. Rev. Lett.* **1992**, *69*, 474.
(8) Retting, W.; Naciri, J.; Shashidhar, R.; Duran, R. S. *Thin Solid Films* **1992**, *210/211*, 114.
(9) Jego, C.; Agricole, B.; Vicentini, F.; Barrouillet, J.; Mauzac, M.; Mingotaud, C. *J. Phys. Chem.* **1994**, *98*, 13408.
(10) Zhu, Y. M.; Lu, Z. H.; Wei, Y. *Phys. Rev. E: Stat. Phys., Plasamas, Fluids, Relat. Interdiscip. Top.* **1994**, *49*, 5316.
(11) Payan, S.; Desbat, B.; Destrade, C.; Nguyen, H. T. *Langmuir* **1996**, *12*, 6627.
(12) Pfeiffer, S.; Shashidhar, R.; Fare, T. L.; Naciri, J. *Appl. Phys. Lett.* **1993**, *63*, 1285.
(13) Xue, Q. B.; Yang, K. Z.; Liu, H. G.; Chen, X.; Jiang, J. Z. *Mater. Sci. Eng., C* **1999**, *10*, 87.
(14) Mu, J.; Okamoto, H.; Yanai, T.; Takenaka, S.; Feng, X. S. *Colloid Surf. A* **2000**, *172*, 87.
(15) Wen, Z.; Jiang, Q.; Tatani, K.; Ozaki, Y. *Zhongnan Gongye Daxue Xuebao* **2005**, *12*, 167.
(16) Yoshihara, T.; Kiyota, Y. *17th ILCC* **1998**, 1−74.
(17) Kawai, T.; Umemura, J.; Takenaka, T. *Langmuir* **1990**, *6*, 672.
(18) Okuyama, K.; Ikeda, M.; Yokoyama, S.; Ochiai, Y. *Chem. Lett.* **1988**, *17*, 1013.
(19) Kawai, T.; Umemura, J.; Takenaka, T. *Langmuir* **1989**, *5*, 1378.
(20) Beveridge, D. L.; Jaffe, H. H. *J. Am. Chem. Soc.* **1966**, *88*, 1948.
(21) McRae, E. G.; Kasha, M. *Physical Processes in Radiation Biology*; Academic Press: New York, 1964.
(22) Kasha, M.; Rawls, H. R.; El-Bayoumi, M. A. *Pure Appl. Chem.* **1965**, *11*, 371.
(23) Chollet, R. A. *Thin Solid Films* **1978**, *52*, 343.
(24) Vandevyver, M.; Barraud, A.; Teixier, R.; Maillard, P.; Gianotti, C. *J. Colloid Interface Sci.* **1982**, *85*, 571.
(25) Kudo, K. *Kiso Bussei Zuhyo*; Kyoritsu Shuppan: Tokyo, Japan, 1972.
(26) Nagasaki, Y.; Yoshihara, T.; Ozaki, Y. *J. Phys. Chem. B* **2000**, *104*, 2846.
(27) Mach, P. *Liq. Cryst. Today* **2002**, *11*, 1.
(28) Zhang, R. F.; Zhang, X.; Li, H. B.; Zhao, B.; Shen, J. C. *Polym. Bull.* **1996**, *36*, 229.
(29) Zhao, B.; Li, H. B.; Zhang, X.; Shen, J. C.; Ozaki, Y. *J. Phys. Chem. B* **1998**, *102*, 6515.
(30) Umemura, J.; Cameron, D. G.; Mantsch, H. H. *Biochim. Biophys. Acta* **1980**, *602*, 32.